Electronic Implementation of High Bandwidth Linear Hydraulic Actuator for Legged Robot ‘s Applications

G. Abdulmalek, A. Ammounah, N. Ait Oukfroukh, S. Alfayad, S. Mammar

Laboratory of Computing, Integrative Biology and Complex Systems (IBISC), Univ Evry, Paris-Saclay University, Evry 91000, France Email: said.mammar@univ-evry.fr

***Abstract*—The Electro-Hydraulic Actuator (EHA) is widely used in various fields, including but not limited to humanoid robotics, industrial actuators, prosthetics, rehabilitation equipment, and aeronautics. The development of legged robots and robotic systems must consider high dynamics and wide bandwidth. Due to their large bandwidth, electro-hydraulic servo valves (EHSV) provide a substantial advantage over traditional electro-hydraulic proportional valves. However, some EHSVs' electrical properties can make it difficult to function correctly. To enhance the dynamic performance of EHSV-based actuation systems, this research suggests a novel electronic driver topology. The hydraulic, electrical, and mechanical components of the Simscape a toolbox in Matlab-Simulink are used to verify the theoretical study that forms the basis of the proposed driver design. Finally, experimental data from a hydraulic system test bench in a lab are acquired.**

***Index Terms*—High Bandwidth Actuators, Dynamic Driver, Servo-valve, Modelling, Current Controller, Torque motor, Electro-Hydraulic Servo-valve (EHSV), Servo-Electro Hydraulic Actuator (SEHA).**

I. Introduction

One of the major issues in robotics research is creating an actuator system for highly dynamic-legged robots. The main criterion needed for highly dynamic tasks is the wide bandwidth of the actuation system [1] [2] [3].

Electric actuators for legged robots can achieve very high bandwidth. These dynamics have been shown in LOLA humanoid robot by achieving 240 Hz for the closed loop joint controller during the typical walking sequence. The servo electronic driver from ELMO Motion Control has been used for each joint. It allows a high sampling rate for feedback [4].

Pneumatic actuators cannot provide high bandwidth compared to electric and hydraulic actuators. This is because of the high compressibility of the air-fluid [5]. Although, some pneumatically actuated robots and bio-inspired muscles have been developed to emulate human muscles [6] [7].
Hydraulic actuation is popular in the industry for heavy-duty applications, but is not very common in robotics. Although, hydraulic actuation has shown the ability for high dynamics performance, such as the ATLAS robot [8], SARCOS CB robot [9], and HyQ2Max [10]. ATLAS robot is the most advanced humanoid robot; it has an impressive dynamic behavior. Unfortunately, very little information is published about the hardware of the robot.

All hydraulic actuated legged robots are developed using hydraulic valves, to control the flow and the pressure.
Different hydraulic valves are available like proportional valves, piezo servo-valves, pipejet, and flapper-nozzle servo-valves.

Proportional valves are more affordable than servo-valves [11]. Some hydraulically actuated robots have used proportional valves, like the lower limb exoskeleton from Virginia Tech [12] and the earlier version of HyQ robot [13]. These examples didn’t show high dynamics performance due to the limited bandwidth of the proportional valve, which doesn’t exceed some tens of Hz [14].
Flapper-nozzle servo valves and pipejet servo-valves are two similar types of valves. They provide fast response and high accuracy in a small size [15]. Both are two-stage servo valves. The first stage is an electrical torque motor.

The Piezoelectric valves are direct one-stage valves. It uses Piezoelectric actuators PEAs instead of the torque motor in the flapper-nozzle and pipejet servo-valves [11]. The PEAs use the inverse effect of the piezo material: it deforms mechanically when applying excitation voltage to it. The material reacts very quickly, which allows obtaining a very high bandwidth for the servo-valve to achieve the range of 1 kHz [16].
The deformation of the piezoelectric material is relatively small (some micrometres). Therefore, most PEAs adopt complex mechanical amplification to increase stroke. As a result, the piezoelectric servo-valves need special electronic drivers, and the size of such drivers is quite extensive. [16].
In our research, we focus on hydraulic actuation by using the flapper-nozzle servo-valves. In the challenge of increasing the response dynamics of the servo-valve-based electrohydraulic actuation, many approaches are proposed in the literature.
One of them suggests using the flow-forward compensation principle. A double valve-control scheme has been used [17]. Another approach is based on the use of a magnetic fluid in the torque motor of the servo-valve. It has been shown that it can increase the responsivity of the torque motor [18]. In our approach, the electrical characteristics of the torque motor of the Moog 30-series and E024-series have been studied, and the electronic driver has been investigated.
The remainder of the paper is organised as follows. Section II is dedicated to the modelling problem of the servo valve. Section III presents the proposed solution, while Section IV

provides the simulation results. Implementation results are detailed in Section V, while Section VI warp-up the paper.

II. DYNAMIC MODEL OF MOOG30 SERIES SERVO-VALVE

A. Principle of Electro-Hydraulic Servo Valve (EHSV)

An electro-hydraulic servo valve is a type of valve used in hydraulic control systems to regulate the flow and pressure of the fluid. There are many servo-valves, but the most common and efficient type is the flapper nozzle servo-valve; the valve uses a flapper and nozzle mechanism, along with a feedback spring, to control the flow of hydraulic fluid and maintain the desired position or velocity of the actuator. [16]

Another critical component of the servo valve is the torque motor coupled with the flapper, which causes it to move and change the flow in the nozzle.

The workflow of the servo valve is as follows:

1- Electrical input: The electric input of the servo valve is the current flow through the torque motor's coils. The current will activate the coils generating a magnetic field. This field acts on a magnetic armature connected to the pivoting arm, causing it to move in a specific direction.

2- Flapper and nozzle mechanism: The nozzle is a small opening through which the fluid flows, and the flapper is a thin, flexible piece of metal attached to a pivoting arm. The current signal controls the position of a flapper within the servo valve. The position of the flapper determines the size of the opening between the nozzles and, therefore, the flow of hydraulic fluid through the valve (internal flow).

3- Main Spool Movement: The valve has a housing with an inlet and outlet port for hydraulic fluid and a spool mounted inside the housing. This spool has several lands (also called spool positions) that can block or allow fluid flow through the valve (from inlet to outlet and vice versa), depending on its position. The flow from the previous stage(flapper-nozzle) will generate a differential pressure on the main spool and make it move.

4- Feedback spring: The hydraulic fluid flows through the valve and is directed to the actuator. At the same time, the position of the flapper is also controlled by a feedback spring. The feedback spring provides a force that opposes the force of the electrical input signal and helps to hold the flapper in position.
This allows the spool to be precisely positioned and held in place by balancing forces between the electrical signal and the spring.
The feedback spring is typically calibrated to provide a specific level of resistance to the movement of the spool. The calibration of the spring is critical for the performance of the servo valve, as it determines the sensitivity and stability of the valve's response to the electrical input signal.

5- Actuator control: The position of the flapper and the size of the opening between the nozzles determine the flow of hydraulic fluid to the actuator, which then moves to the desired position or velocity. As the actuator moves, it sends a feedback signal back to the control system, which can be used to adjust the electrical input signal and maintain the desired position or velocity.

The typical operational parts of the studied servo-valve and the principle of operation are shown in Figure 1. [16]

In conclusion, the EHSV consists mainly of two stages; the first stage is a torque motor with a flapper nozzle, and the second stage is a standard four-spool valve [19].

B. Dynamic model Problem

Although the simplicity of its working principle (as explained above), the servo valve is considered a very complex system when we are trying to derive a control model because three domains of science are concerned in this system Mechanics, Hydraulics, and Electrics.

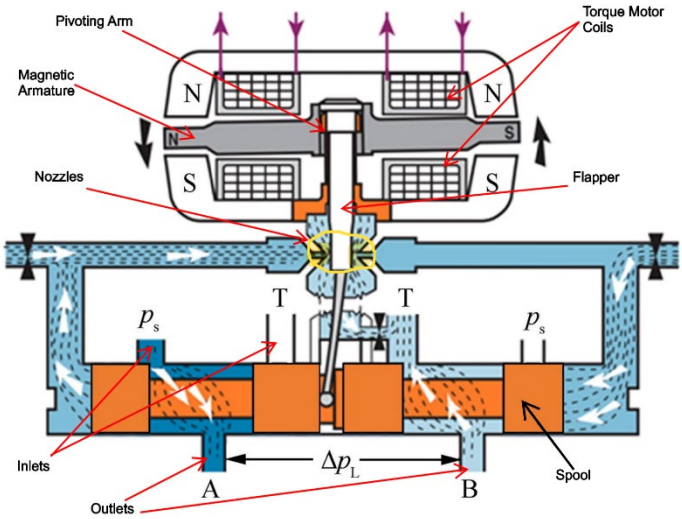

Figure 1 EHSV Working Principle

Many works have been done to have a good model representing the servo valve [20], [21].

Although much work is done for EHSV modelling, they all start with the electric current as input for such a system, as shown in Figure 2 [22], which supposes the ideal behavior of the torque motor and ignores the current dynamics caused by the high values of the motor inductance and resistor.

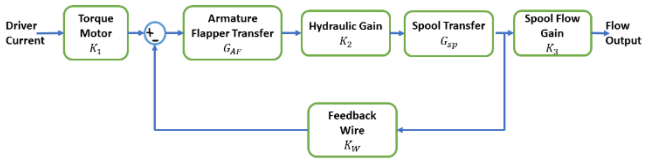

Figure 2 Servo Valve Dynamic Model Block Diagram*[5]

To better explain this problem, let's consider the simplified (see Appendix2) servo-valve block diagram shown in Figure 2 [23], if we keep the torque motor as just a gain, we can write:

$$G_{AF}(p) = \frac{\left(\frac{1}{K_f}\right)}{1+\left(\frac{2\xi}{\omega_n}\right)p+\left(\frac{p}{\omega_n}\right)^2} \quad (1)$$

$$G_{sp}(p) = \frac{1}{Ap} \quad (2)$$

Considering the control block diagram Figure 2 and the equations (1) and (2), we can express the current (in mA) to flow (in^3/sec) transfer function as in equation (3)

$$\frac{Q_v}{i} = \frac{\alpha}{\frac{A}{{\omega_n}^2}p^3 + A\left(\frac{2\xi}{\omega_n}\right)p^2 + Ap + \beta} \quad (3)$$

$$where \left\{\alpha = \frac{K_1 K_2 K_3}{K_f}, \beta = \frac{K_W \cdot K_2}{K_f}\right\}.$$

Now, if we consider the current dynamic of the torque motor and add it to the control block diagram, as shown in Figure 3, we can obtain the following transfer function.

$$\frac{Q_v}{u} = \frac{\alpha}{\frac{A}{{\omega_n}^2}p^3 + A\left(\frac{2\xi}{\omega_n}\right)p^2 + Ap + \beta}\frac{\alpha_i}{1+\beta_i p} \quad (4)$$

$$where \quad \alpha_i = \frac{1}{R} and \beta_i = \frac{L}{R}$$

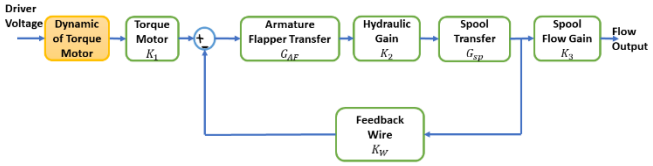

Figure 3 Servo Valve Model considering the electric current Dynamics

Simulating the two transfer functions equations (3) and (4) with the same step input, we get the result shown in Figure 4

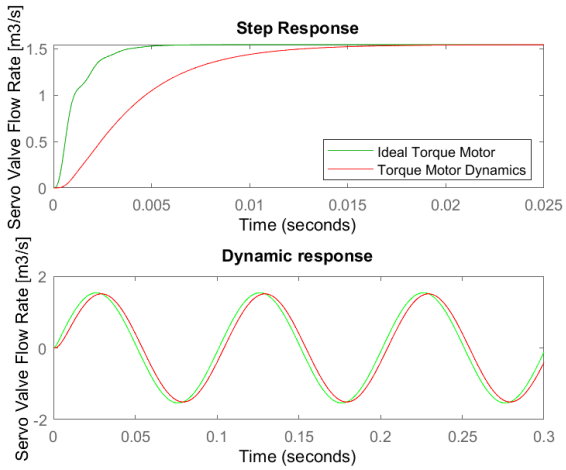

Figure 4 Servo Valve Step Response (Green: Ideal Torque Motor, Red: Current Dynamic of the Torque motor is considered)

We notice clearly the high impact the dynamics of the torque motor on the servo valve dynamic behavior, where the settling time in the ideal torque motor case (the green curve) and for the case where the torque motor dynamic is considered (the red curve) $T_{Torque\_s} = 10.8ms$ which is three times greater than the ideal case. The responses for a 10Hz sinusoid input leads to a 10 *ms* time delay.

III. Proposed Solution

Considering the high impact of the current dynamic of the torque motor on the total EHSV system settling time which directly affects the dynamics of the robot's movement, we propose a new dynamic driver topology to overcome this problem and enhance the current dynamics of the torque motor, hence improving the total EHSV system's dynamics.

A. Proposed High Dynamic Driver

Figure 6 shows the schematic of our proposed high dynamic driver, with $V_{DD} = +72V$ *and* $V_{SS} = -72V$.

A.1 Linear Analysis of the Driver

Analyzing the driver circuit linearly, we find that the output of the driver can be described by equation (5).

$$u = \frac{1}{R_f C_f}\int v_c - \frac{R_s}{R_f C_f}\int i_s + v_c - R_s i_s \quad (5)$$

Defining the reference current to be $i_{ref} = \frac{v_c}{R_s}$ we can rearrange the last equation as follows:

$$u = \frac{R_s}{R_f C_f}\int \left(\frac{v_c}{R_s} - i_s\right) + R_s\left(\frac{v_c}{R_s} - i_s\right)$$

$$\Rightarrow u = K_i \int (i_{ref} - i_s) + K_p(i_{ref} - i_s) \quad (6)$$

$$where\ K_p = R_s, K_i = \frac{R_s}{R_f C_f}$$

Apply Laplace transform to equation (6) we got the equation (7)

$$U(p) = \frac{K_i}{p}E(p) + K_p E(p) \quad (7)$$

$$where\ E(p) = I_{ref}(p) - I_s(p)$$

So, a linear analysis view shows that our current controller has the behavior of a proportional integral controller.

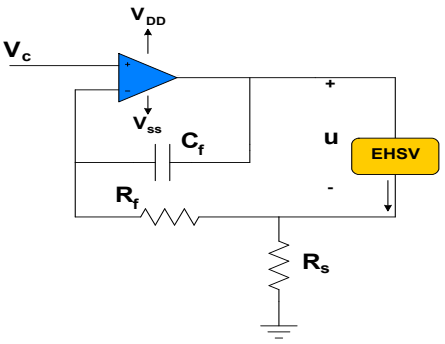

Figure 5 High Dynamic Driver Proposed Schematic

A.2 Nonlinear analysis of the Driver

Saturation effects occur when any part of a feedback control system reaches a physical limit. And this is precisely what happens with an operational amplifier where the output voltage is limited to a value near the supply voltage.

Since our current driver is established using an operational amplifier, then we have the saturation effect, which could be expressed as

$$V_o = \begin{cases} +V_{sat} if V_{in+} > V_{in-} \\ -V_{sat} if V_{in+} < V_{in-} \end{cases} \quad (7)$$

In fact, the saturation effect of our driver will appear in the transient state where the speed change in the current is needed, as we will see in the simulation.

IV. SIMULATION RESULTS

A. Current Control Loop

To validate the dynamic behavior the proposed driver topology, we build a hydraulic cylinder system with mechanical load and with the proposed servo valve model in Simscape toolbox (Simhydraulics, Simmechanics) / MATLAB Simulink as shown in Figure 6.

The driver circuit is itself built using SimElectrical toolbox and limited bandwidth OP-AMP with ±72 Volt as rail supply- (Figure 7).

As shown in Figure 8, the driver output is the op amp voltage saturation $u \simeq V_{DD} = +72V$ for the transient phase.

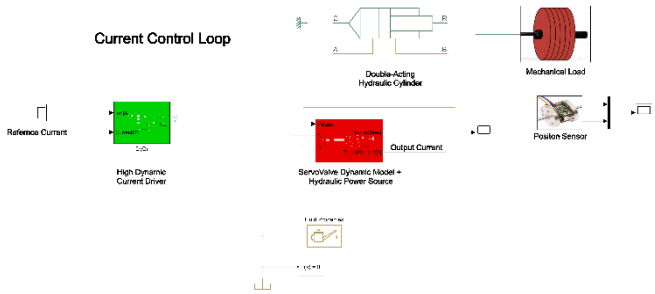

Figure 6 Simscape simulation for the Hydraulic System, Servo Valve and Driver

The error between the desired current value and the actual current is very high, but when the actual current gets close to the desired value, we clearly see the linear behavior of the driver.

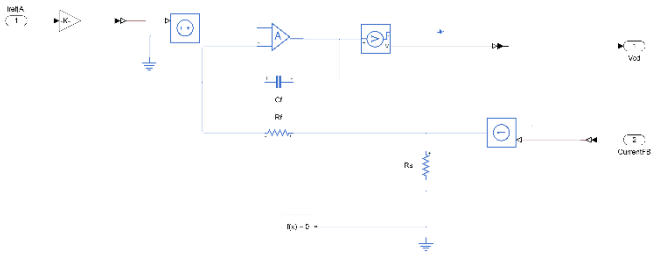

Figure 7 Driver Circuit in SimElectrical

And in total, we got 0.5 ms as settling time for the current.

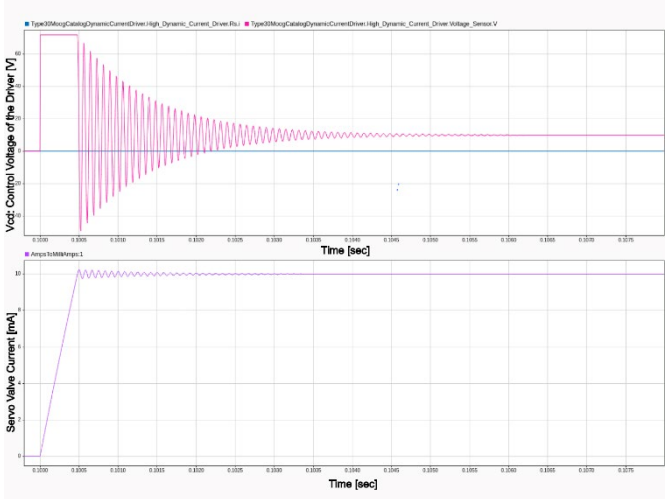

Figure 8 Current Dynamic (Down-Purple) and Driver Output Voltage (Up-Red)

B. Double Control Loop – Flow and Current

To verify the enhancement impact of our driver on the flow control loop, we simulate the flow control loop using a PID controller, as shown in Figure 9.

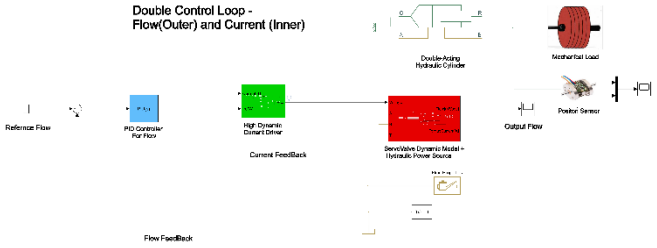

Figure 9 Flow Control Loop (Outer) and Current Control Loop (Inner) in Simulink

Our main objective here is to examine the servo-valve flow-settling time, so we did not optimize the PID parameter to obtain the fastest possible response, but we tuned the PID parameter to have acceptable performance in order just to compare the two cases:

1. The settling time of the flow response using the proposed high dynamic high voltage driver.
2. The settling time of the flow response using a low voltage driver.

Figure 10 shows the flow step response of the servo-valve with a step value corresponding to the nominal flow for the Moog30 servo-valve $0.2\,X\,10^{-3}\ m^3/s$, using the proposed high voltage driver, we observe that the settling time is $3.3\,ms$.

For the sake of better comparison, we placed the flow step response with the same condition just after in Figure 11, where we can observe a $6\,ms$ of settling time, which means that the high voltage driver enhances the flow control loop speed by 181%.

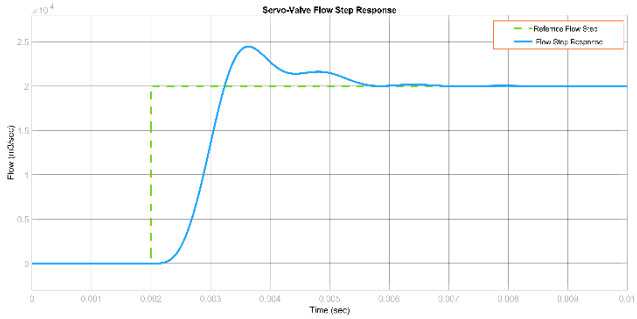

Figure 10 Flow Step Response with High Dynamic Current Driver(181 % speed enhancement)

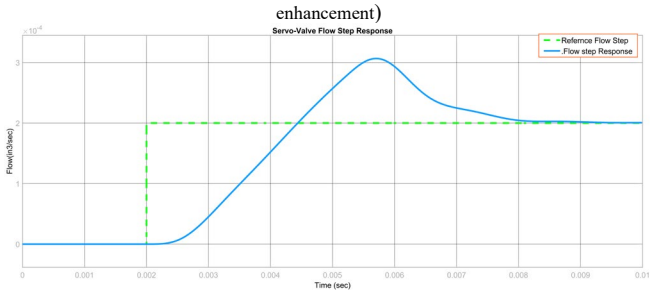

Figure 11 Serov-Valve Flow Step Response with Low Dynamic Current

V. IMPLEMENTATION AND EXPERIMENTAL RESULTS

To test the driver, we implement the hydraulic circuit as shown in Figure 12 and Figure 13.

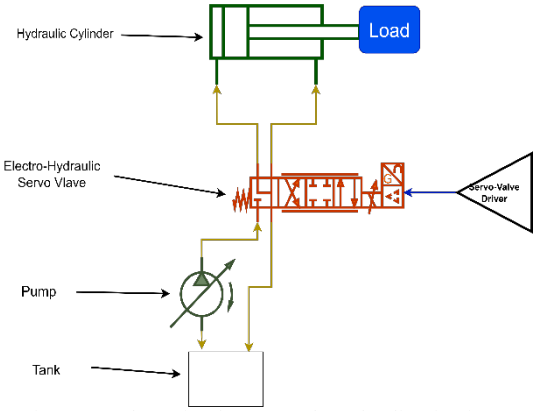

Figure 12 Schematic of Test Bench Hydraulic Circuit

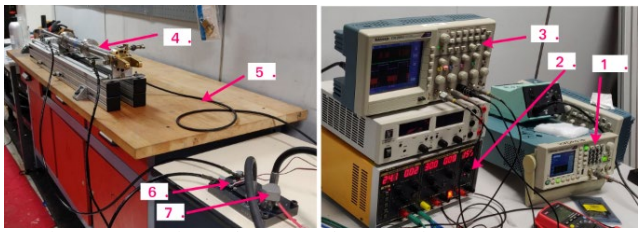

Figure 13 Experimental Test Bench (1-Function Generator 2- Power Supply 3- Scope 4-Hydraulic Cylinder 5- Position Sensor 6- Pressure Sensor 7-EHSV)

To observe the enhancement in the current dynamics, the results of our driver (Figure 14) are compared to two other drivers:

1- Off the shelf industrial driver My-502.
2- Developed H-bridge-based topology driver.

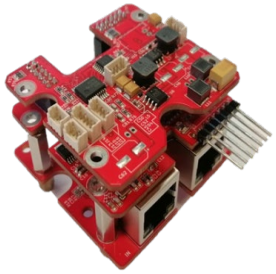

Figure 14 Our Developed high-voltage dynamic driver*

A. *Experimental Results*

First, the current response of the servo-valve is measured using the industrial driver My-502, and it is shown in Figure 15 that the response represents $\pm 5mA$.

The measured settling time is, $T_{My502\_s} = 5ms = 0.5T_{Torque\_s}$.

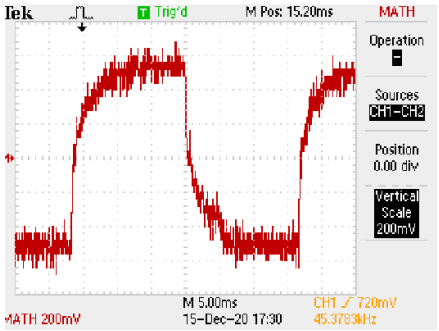

Figure 15 Step response of the commercial driver MY-502

Second, the H-bridge topology-based driver with digital PID implementation is tested, and we got the current step response shown in Figure 16(the response represents $\pm 5mA$.

The measurement of the current settling time gives:

$$T_{Hbridge\_s} = 2ms \pm 0.18 * T_{Torque\_s}$$

Figure 16 Step Response of H-Bridge-based Driver

Finally, our proposed driver is tested under the identical experimental conditions. The achieved step response is shown in Figure 17.

Figure 17 Step Response of Proposed Driver

The measured settling time in this case is

$$T_{HighDynamic\_s} = 0.25ms = 0.02 * T_{Torque\_s}$$

Our control has thus enhanced the settling time.

VI. CONCLUSION AND FUTURE WORK

In this study, a driver is developed that improves the dynamics of the servo-valve system by speeding up the current control and even allows controller designers to utilize any model (4)(5) because utilizing such driver topology renders knowledge of the current dynamics irrelevant.

The current control loop becomes fifty times faster than the flow outer loop when the proposed driver is used in the EHSV control system.

Additionally, since the servo-valve does not require a large driving current (in the milliamp range), the H-bridge Topology is not required, and the high supply OP-AMPS technique is a very practical one for the driver design.

Other actuators, like the SEHA actuator, can be driven using the suggested method to improve dynamics, in addition to the servo valve-based actuation system [24].

To continue our study in the future, the position and flow control loops will be implemented following the improvement and implementation of the current control loop in order to compare the actual results with those from the simulation.

Driver Type	Current Settling Times[ms]
My502 Industrial Driver	$5ms = 50\% * T_{Torque\_s}$
H Bridge Topology	$2ms = 18\% * T_{Torque\_s}$
Proposed Op amp Driver	$0.25ms = 2\% * T_{Torque\_s}$

APPENDIX

VII. APPENDIX A. SYMBOLS

Symbol	Definition	Value for MOOG30 servo valve
i	The current of Torque Motor	$\pm 10mA$
Q_v	Hydraulic Amplifier Differential flow	$\pm 4\ gpm$
X_s	Spool Displacement	$\pm 0.015\ in$
K_W	Feedback Wire Stiffness	$16.7\ in-lbs/in$
K_1	Torque Motor Gain	$0.025\ in-lbs/mA$
K_2	Hydraulic Amplifier Flow Gain	$150\ \frac{in^3/\sec}{in}$
K_3	Flow Gain of Spool/Bushing	$1030\ \frac{in^3/\sec}{in}$
K_f	Net Stiffness on Flapper/Armature	$115\ in-lbs/in$
A	Spool End Area	$0.026\ in^2$
ξ	Damping Ratio of the First Stage	0.4
ω_n	Natural Frequency of the First Stage	$814Hz$
L	Torque Motor Coil Inductance	$3.2H$
R	Torque Motor Coil Resistance	1000Ω

VIII. APPENDIX B. ASSUMPTIONS FOR THE MODEL

This model is derived under the following assumptions:
1-An ideal current source (infinite Impedance) is used.
2- Negligible load pressure exists.
3-All nonlinearities can either be approximated by linear dynamic effects or can be neglected.
4-The armature/flapper can be represented as a simple lumped-parameter system.
5-Perturbation conditions can be applied to the hydraulic amplifier orifice characteristics.
6- Fluid compressibility and viscosity effects are negligible.
7- Motions of the flapper are small concerning spool motion.
8-The forces necessary to move the spool are small concerning the driving force available.

CONFLICT OF INTEREST

The authors declare no conflict of interest.

AUTHOR CONTRIBUTIONS

G. Abdulmalek conducted the research together this work with A. Ammounah. N. Ait Oufroukh worked more specifically on the electronic part while S. Alfayad contributed on the hydraulic aspects. S. Mammar makes suggestions on the control and simulation part. All the authors contributed to the different parts of the paper and all authors had approved the final version.

ACKNOWLEDGMENT

This work was supported by the PAUSE Program, KALYSTA, and SATT Paris-Saclay.

REFERENCES

[1] Wensing, P.M., Wang, A., Seok, S., Otten, D., Lang, J., and Kim, S. (2017). Proprioceptive Actuator Design in the MIT Cheetah: Impact Mitigation and High-Bandwidth Physical Interaction for Dynamic Legged Robots. IEEE Transactions on Robotics. 509-522. doi:10.1109/TRO.2016.2640183

[2] Stasse, O., and Flayols, T. (2019). An Overview of Humanoid Robots Technologies. In: Venture, G., Laumond,J.P., and Watier, B., (ed.). Biomechanics of Anthropomorphic Systems. 281-310. Springer Tracts in Advanced Robotics. Springer International Publishing. doi:10.1007/978-3-319-93870-7_13

[3] Sugihara, T., & Morisawa, M. (2020). A survey: dynamics of humanoid robots. Advanced Robotics. 1338–1352. doi:10.1080/01691864.2020.1778524

[4] Sygulla, F., Wittmann, R., Seiwald, P., et al. (2018). An EtherCAT-Based Real-Time Control System Architecture for Humanoid Robots. IEEE 14th International Conference on Automation Science and Engineering (CASE). 483-490. doi:10.1109/COASE.2018.8560532

[5] Versluys, R., Deckers, K., Van Damme, M., et al. (2009). A Study on the Bandwidth Characteristics of Pleated Pneumatic Artificial Muscles. Applied Bionics and Biomechanics. 3-9. doi:10.1080/11762320902738647

[6] Ahmad Sharbafi, M., Shin, H., Zhao, G., Hosoda, K., and Seyfarth, A. (2017). Electric-Pneumatic Actuator: A New Muscle for Locomotion. Actuators. doi:10.3390/act6040030

[7] Vanderborght, B., Verrelst, B., Van Ham, R., Van Damme, M., and Lefeber, D. (2005). A pneumatic biped: experimental walking results and compliance adaptation experiments. 5th IEEE-RAS International Conference on Humanoid Robots. 44-49. doi:10.1109/ICHR.2005.1573543

[8] Nelson, G., Saunders, A., and Playter, R. (2019). The PETMAN and Atlas Robots at Boston Dynamics. In Vadakkepat, P. (ed.) Humanoid Robotics. 169-186. Springer, Dordrecht. doi:10.1007/978-94-007-6046-2_15

[9] Cheng, G., Hyon, S.H., Morimoto, J., et al. (2007). CB: a humanoid research platform for exploring neuroscience. Advanced Robotics. 1097-1114. doi:10.1163/156855307781389356

[10] Semini, C., Goldsmith, J., Rehman, B.U., Frigerio, M., Barasuol, V., Focchi, M. and Caldwell, D.G. (2015). Design overview of the hydraulic quadruped robots HyQ2MAX and HyQ2CENTAUR. 14th Scandinavian International Conference on Fluid Power. Tampere, Finland, 20-22.
[11] Plummer, A. (2016). Electrohydraulic servovalves – past, present, and future. Proc 10th International Fluid Power Conference. 405-424.
[12] Yang, J. (2017). Design and experiment of the lower extremity exoskeleton. IEEE 2nd Advanced Information Technology, Electronic and Automation Control Conference (IAEAC). 1380-1383. doi:10.1109/IAEAC.2017.8054240
[13] Semini, C., Tsagarakis, N.G., Guglielmino, E., Focchi, M., Cannella, F., and Caldwell, DG. (2011). Design of HyQ – a hydraulically and electrically actuated quadruped robot. Proceedings of the Institution of Mechanical Engineers, Part I: Journal of Systems and Control Engineering. 831-849. doi:10.1177/0959651811402275
[14] Sarkar, B.K., Das, J., Saha, R., Mookherjee, S., and Sanyal, D. (2013). Approaching Servoclass Tracking Performance by a Proportional Valve-Controlled System. IEEE/ASME Transactions on Mechatronics. 1425-1430. doi:10.1109/TMECH.2013.2253116
[15] Xuan Hong Son, P., and Thien Phuc, T. (2017). Comparison of jet pipe servo valve with flapper nozzle servo valve. Science and Technology Development. 78-83. doi:10.32508/stdj.v20iK1.418
[16] Tamburrano, P., Sciatti, F., Plummer, A.R., Distaso, E., De Palma, P., and Amirante, R. (2021). A Review of Novel Architectures of Servovalves Driven by Piezoelectric Actuators. Energies. 4858. doi:10.3390/en14164858
[17] Bai, Y., and Quan, L. (2013). New method to improve dynamic stiffness of electro-hydraulic servo systems. Chin J Mech Eng. 997–1005. doi:10.3901/CJME.2013.05.997
[18] Li, S., and Song, Y. (2007). Dynamic response of a hydraulic servo-valve torque motor with magnetic fluids. Mechatronics. 442–447. doi:10.1016/j.mechatronics.2007.04.011
[19] Fales, R. C., and Manring, N. D. (2020). Hydraulic control systems. Wiley. 155-224. doi.org/10.1002/9781119418528.ch4
[20] Xu, Y. (2013). Modelling and Control of a High Performance Electro-Hydraulic Test Bench. HAL. INSA de Lyon.
[21] Xu, Y., Bideaux, E., Sesmat, S., Sidhom, L., and Brun, X. (2010). Hydro-Mechanical Model of Electro-Hydraulic Servovalve Based on Bond Graph. 6th Fluid Power Net International PhD Symposium. hal-00988577.
[22] MOOG. (2019a). TYPE 30 NOZZLE-FLAPPER FLOW CONTROL SERVOVALVES //www.moog.com/industrial
[23] MOOG. (2019b). 30 SERIES MICRO SERVO VALVES,30 Series Servo Valves /TJW / Rev. G, Id. CDL45964-en.//www.moog.com/industrial
[24] Alfayad S., Kardofaki M., Sleiman M., (2020) Hydraulic Actuator with Overpressure Compensation. WO Patent No. 2020173933. International office